Available online at www.sciencedirect.com
SCIENCE DIRECT®
ELSEVIER
International Journal of Solids and Structures 41 (2004) 6317–6333
INTERNATIONAL JOURNAL OF SOLIDS and STRUCTURES
www.elsevier.com/locate/ijsolstr

Size-dependent elastic fields of embedded inclusions in isotropic chiral solids

P. Sharma *

Department of Mechanical Engineering, University of Houston, Houston, TX 77204, USA

Received 8 December 2003; received in revised form 26 April 2004
Available online 17 June 2004

Abstract

A chiral solid exhibits handedness i.e. broken reflection or mirror symmetry. In the present work, utilizing the concept of a hemitropic micropolar medium, Eshelby's classical elastic treatment of embedded inclusions is extended to chiral solids. Unlike the classical elastic case, in addition to exhibiting chirality, the derived "chiral Eshelby tensors" are size-dependent exhibiting a characteristic length scale related to the inclusion size. Closed-form results are presented for the spherical and circular cylindrical shape. In a chiral solid even a purely dilating inclusion exhibits microrotations and moment stresses. Such an effect has no counterpart in classical elasticity or even in the conventional indeterminate couple stress and centrosymmetric micropolar theories. In fact, the latter yields just the classical elastic results for pure dilatation problems. Unlike the classical elastic case, the modified Eshelby tensors for chiral solids are inhomogeneous within the interior of the inclusion. The present work is likely to find applications in diverse areas such as biological inclusions, inhomogeneities in structures such as wood, foams, chiral sculptured thin films, bones and other complex materials exhibiting axial–twist coupling.

1. Introduction

In mechanics of materials one distinguishes between material properties depending upon orientation. A fully isotropic material, for example, is completely invariant under proper orthogonal rotations. Although rarely stated but tacitly implied is also the invariance of the classical elastic material behavior under mirror reflections. Thus even a completely anisotropic classical elastic solid exhibits no"handedness" or chirality. As well-known in condensed matter theory (Marder, 2000) effects like piezoelectricity necessarily require chirality (see also, Lakes, 2001). Chiral materials are said to lack centrosymmetry and are often referred to as non-centrosymmetric materials.

* Tel.: +1-7137434500; fax: +1-7137434503.
E-mail addresses: psharma@uh.edu, psharma@nanomechanics.org (P. Sharma).

0020-7683/$ - see front matter © 2004 Elsevier Ltd. All rights reserved.
doi:10.1016/j.ijsolstr.2004.05.004

Several naturally occurring materials are essentially chiral in nature e.g. DNA (Haijun and Zhong-can, 1998), bone (Lakes, 1981), wood, quartz (Lakes, 2001) and certain types of carbon nanotubes (Harris, 2002). Fabricated structures such as foams, chiral sculptured thin films (Robbie et al., 1996), materials with helical inclusions, and twisted fibers (Lakes, 1981, 2001) also appear to exhibit chiral behavior. In these and other such materials, chirality manifests itself in various interesting and technologically relevant forms e.g. chiral sculptured thin films are of importance in selected optoelectronics applications (Robbie et al., 1996). In the context of elastodynamics, recently, Ro (1999) has predicted Cotton effect in chiral elastic solids. It is worth mentioning here that certain types of recently fabricated artificial composites that show negative refractive index in selected frequency range (thus effectively inverting phenomena such as Doppler's effect) are often termed "left-handed" materials (Smith et al., 2000). The reader is referred to McCall et al. (2002) for detailed clarifications, however, the aforementioned behavior has no relation to chirality and the moniker of "left-handed" material is an unfortunate misnomer, thus often confounding researchers (including, in the past, the present author).

Insofar as elasto-statics is concerned (which is the scope of the present work), chirality can be best visualized by embodying the material with a screw-like character e.g. a solid may exhibit torsion under axial stretch (Fig. 1). Biological materials and inclusions such as DNA and certain proteins dedicate part of their (even purely) hydrostatic strain energy to curvatures. To provide further visualization of chirality in static linearized elasticity, we qualitatively contrast the response of a circular cylindrical rod to a homogeneous axial stress in Fig. 1 for four classes of materials: (i) an isotropic classical solid, (ii) a completely anisotropic classical solid, (iii) a micropolar elastic material and (iv) an isotropic chiral solid (i.e. hemitropic micropolar medium). As depicted, the cylindrical rod for the isotropic case will simply exhibit tensile stresses (i.e. no shear deformations are present and the elastic state is homogeneous). The stress state is symmetric and couple stresses are absent ($m_{ij} = 0$). In the second case, where the material has the most generalized anisotropy allowed by classical elasticity, we now note also the presence of shear deformations although the elastic state is still homogeneous. In the third case, the material is an isotropic centrosymmetric micropolar material. The response (qualitatively) is exactly as of classical isotropic elasticity for this particular simple example. Finally, the fourth case that is shown in Fig. 1 is of an isotropic chiral solid. In the latter case, the cylindrical rod will exhibit an inhomogeneous elastic state (i.e. twist or torsion) in addition to the tensile behavior one would expect from a classical or even centrosymmetric micropolar solid. Couple stresses are

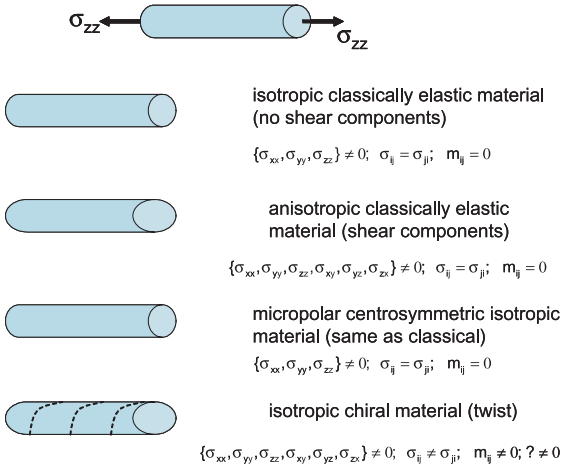

Fig. 1. Elucidation of chirality in static elasticity.

also present (i.e. $m_{ij} \neq 0$). The reader is referred to Lakes and Benedict (1982) and Lakes (2001) for a more quantitative discussion of the fourth case. Suffice to say that the twisting behavior of a solid under an axial stress is a purely chiral phenomenon and has no counterpart in classical elasticity regardless of the anisotropy.

Keeping in mind the aforementioned developments in chiral materials, in the context of *classical* elasticity, Eshelby's solution of an embedded inclusion (Eshelby, 1957, 1959, 1961) is of fundamental importance in materials science, mechanics, solid state physics and is frequently invoked in diverse areas and problems of physical sciences, e.g. localized thermal heating, residual strains, dislocation-induced plastic strains, phase transformations, overall or effective elastic, plastic and viscoplastic properties of composites, damage in heterogeneous materials, quantum dots, microstructural evolution; to name just a few. While the literature on Eshelby's tensor (for inclusions) and related problems is indeed rich and extensive no effort, it appears, has been made towards extending his originally classical elastic formalism to chiral solids. In the present work, by simulating isotropic chiral solids via the concept of a hemitropic micropolar material, we seek to present the complete solution to the elastic problem of a transforming chiral inclusion located in a chiral solid. The resulting modified Eshelby tensors (which are four in number in contrast to one in classical elasticity) exhibit both chirality as well as a size-dependency missing, of course, in classical elasticity.

Hemitropic micropolar media has been well recognized to represent chirality in materials e.g. (Lakes, 1981, 2001; Ro, 1999; Lakhtakia et al., 1988; Lakes and Benedict, 1982; Nowacki, 1977, 1986). A micropolar solid admits independent microrotation degrees of freedom in addition to the classical displacements. An excellent, and reasonably current, update on micromorphic theories is presented by Eringen (1999). Some early pioneering work in chiral solid mechanics is due to Nowacki (1977) who first presented the Green's function for an infinite media. Some other relevant results are also summarized in Nowacki (1986). Lakes and Benedict (1982) present a good overview of hemitropic micropolar elasticity and discuss, as an example, torsion of a cylinder. Several elasto-dynamic problems have also been solved. The reader is referred to the paper by Lakhtakia et al. (1988) who discuss the dispersion and field equations of hemitropic medium. Their paper also contains a reference list fairly current until that year. More recently, Lakes (2001) has presented an overview of the subject where simple instructive examples illustrating chirality as well as micropolar effects in deformation of slabs and plates are discussed. In an interesting paper, Lakhtakia (2002) while still employing classical elasticity, incorporates chirality in sculptured thin composite films via local homogenization and introduction of empirical constants. With the exception of the few already mentioned, most solutions of micropolar elasticity have been restricted to the non-chiral (centrosymmetric) case. For example, while tremendous amount of work has been done on inclusion problems in classical elasticity (e.g. Bilby et al., 1984; Mura, 1987; Mura et al., 1996; Mura, 2000; Markov and Preziosi, 2000), there appear to be only three papers (Cheng and He, 1995, 1997; Sharma and Dasgupta, 2002) on Eshelby's inclusion problem in micropolar elasticity—all three adopt a centrosymmetric micropolar media thus excluding chirality. The pioneering works of Cheng and He (1995, 1997) presented micropolar Eshelby tensors for spherical and cylindrical inclusions respectively while predicated on their work, Sharma and Dasgupta (2002) derived closed-form expressions for the overall size-dependent elastic properties of micropolar composites. In summary, the analogue of Eshelby's inclusion solution in hemitropic micropolar (isotropic chiral) medium does not exist which is the object of this work. Applications are anticipated in complex structures such as composite thin films, bones, DNA, nanotubes among others.

In Section 2, the equations of the hemitropic micropolar medium are formulated while the general inclusion problem is tackled in Section 3. Closed-form analytical results are obtained for spherical and infinite circular cylindrical inclusions in Section 4. To bring about clearly the effect of chirality in the context of inclusions, we present several numerical results in Section 5 concluding finally with a summary in Section 6.

2. Fundamental problem formulation of isotropic chiral (hemitropic micropolar) media

As indicated earlier, in a hemitropic media, the conventional assumption of centrosymmetry is abandoned. In addition, beyond the classical displacement degrees of freedom each material point (like in the centrosymmetric micropolar media) is endowed with independent microrotations to both which the material responds through regular (force) stresses and couple stresses.

Both boldface and index notation will be used as convenient. The following kinematic relations relate curvature (or torsion) and strain tensors to the displacement and microrotations vectors:

$$\begin{aligned}\boldsymbol{\Sigma} &= (\nabla \otimes \mathbf{u})^{\mathrm{T}} - \boldsymbol{\epsilon}\boldsymbol{\phi} \\ \mathbf{K} &= (\nabla \otimes \boldsymbol{\phi})^{\mathrm{T}}\end{aligned} \tag{1a–b}$$

Here, $\boldsymbol{\Sigma}$ is the strain tensor while $\mathbf{K}$ is the curvature tensor. $\mathbf{u}$ and $\boldsymbol{\phi}$ represent displacement and microrotation vectors respectively. $\boldsymbol{\epsilon}$ is the permutation tensor. Unless otherwise noted, all tensors are Cartesian and repeated indices indicate summation. Isotropy and linearized relations are assumed throughout. A single dot indicates contraction with respect to one index while a colon indicates contraction with respect to two indices.

Based upon the axiom of invariance of the energy balance law to the Galilean transformation group, the balance laws can be derived (Eringen, 1999):

$$\begin{aligned}&\operatorname{div}\boldsymbol{\sigma} + \mathbf{F} = 0 \\ &\boldsymbol{\varepsilon} : \boldsymbol{\sigma} + \operatorname{div}\mathbf{m} + \mathbf{M} = 0\end{aligned} \tag{2a–b}$$

Here $\boldsymbol{\sigma}$ is the stress tensor, which is generally asymmetric, and $\mathbf{m}$ is the moment stress tensor. $\mathbf{F}$ and $\mathbf{M}$ are, respectively, body force and moment densities. So far, the preceding equations are identical to those of centrosymmetric micropolar elasticity. Chirality is now introduced via the constitutive equations:

$$\begin{aligned}\boldsymbol{\sigma} &= \mathbf{a} : \boldsymbol{\Sigma} + \mathbf{b} : \mathbf{K} \\ \mathbf{m} &= \mathbf{b}^{\mathrm{T}} : \boldsymbol{\Sigma} + \mathbf{c} : \mathbf{K}\end{aligned} \tag{3a–b}$$

Here $\mathbf{a}$, $\mathbf{b}$ and $\mathbf{c}$ are the fourth order hemitropic stiffness tensors. In centrosymmetric micropolar materials, the stiffness tensors are invariant under mirror reflections thus requiring that $\mathbf{b}$ vanish. To contrast centrosymmetric and hemitropic materials, both property sets are written explicitly below (Nowacki, 1977, 1986):

$$\begin{aligned}&\text{Centrosymmetric micropolar media:} \\ &a_{jikl} = (\mu+\alpha)\delta_{jk}\delta_{il} + (\mu-\alpha)\delta_{jl}\delta_{ik} + \lambda\delta_{ij}\delta_{kl} \\ &b_{jikl} = 0 \\ &c_{jikl} = (\gamma+\varepsilon)\delta_{jk}\delta_{il} + (\gamma-\varepsilon)\delta_{jl}\delta_{ik} + \beta\delta_{ij}\delta_{kl} \\ &\text{Hemitropic micropolar media:} \\ &a_{jikl} = (\mu+\alpha)\delta_{jk}\delta_{il} + (\mu-\alpha)\delta_{jl}\delta_{ik} + \lambda\delta_{ij}\delta_{kl} \\ &b_{jikl} = (\chi+\nu)\delta_{jk}\delta_{il} + (\chi-\nu)\delta_{jl}\delta_{ik} + \kappa\delta_{ij}\delta_{kl} \\ &c_{jikl} = (\gamma+\varepsilon)\delta_{jk}\delta_{il}(\gamma-\varepsilon)\delta_{jl}\delta_{ik} + \beta\delta_{ij}\delta_{kl}\end{aligned} \tag{4a–f}$$

Here we note that three additional material constants (to those of centrosymmetric media) χ, κ and ν are needed to describe a chiral solid. ε, α and γ are the three conventional micropolar constants required to describe a centrosymmetric micropolar media in addition to the classical Lame′ constants, μ and λ. Along with the appropriate boundary conditions, Eqs. (1)–(4) complete the *static* boundary value problem definition for both centrosymmetric and hemitropic media.

Through algebraic manipulation, the final static Navier-like governing equations for the hemitropic solid can be written conveniently as:

$$(\mu+\alpha)\nabla^2\mathbf{u}+(\mu+\lambda-\alpha)\text{grad}\,\text{div}\,\mathbf{u}+2\alpha\text{curl}\,\boldsymbol{\phi}+\underline{(\chi+v)\nabla^2\boldsymbol{\phi}+(\kappa+\chi-v)\text{grad}\,\text{div}\,\boldsymbol{\phi}}+\mathbf{F}=0$$
$$(\gamma+\varepsilon)\nabla^2\boldsymbol{\phi}-4\alpha\boldsymbol{\phi}+(\beta+\gamma-\varepsilon)\text{grad}\,\text{div}\,\boldsymbol{\phi}+2\alpha\text{curl}\,\mathbf{u}$$
$$+\underline{4v\text{curl}\,\boldsymbol{\phi}+(\chi+v)\nabla^2\mathbf{u}+(\kappa+\chi-v)\text{grad}\,\text{div}\,\mathbf{u}}+\mathbf{M}=0 \tag{5a–b}$$

Following Nowacki's lead (1986), we have underlined the relevant parts of Eqs. (5) that appear due to the presence of chirality. We note here that there is a minor typographical error in Nowacki's (1977) presentation of Eqs. (5). In absence of the underlined terms, Eqs. (5) reduce to those of centrosymmetric micropolar elasticity (Eringen, 1999).

3. The general inclusion problem in chiral solids

Consider a localized (and for now) an arbitrarily shaped region (Ω) in an infinite linear elastic material (D) undergoing a uniform stress-free inelastic strain (Σ^*) and torsion (K^*) (Fig. 2). Such stress–free strains are referred to as either transformation strains (Eshelby, 1957) or eigenstrains (Mura, 1987). The concept of eigentorsions was introduced by Cheng and He (1995) in exact analogy to eigenstrains. Various physical examples of such strains and torsions are those resulting from thermal expansion, dislocation and disclination mediated inelastic deformations, magneto–electro-mechanical deformations, linear and rotational lattice mismatch and so forth. If the inclusion is removed from the material and allowed to relax (thus enacting the eigenstrain or eigentorsion), no stresses or moments are generated. However, due to the presence of the matrix or surrounding material, the final relaxed elastic state of the inclusion admits a state of stress and moment. When the material properties of the inclusion and the matrix are the same, the problem of determining the elastic state is often referred to as Eshelby's first problem. The scenario where the inclusion elastic properties are different than those of the matrix is Eshelby's second problem (in which case the inclusion is referred to as an "inhomogeneity"). This nomenclature was introduced by Mura (1987).

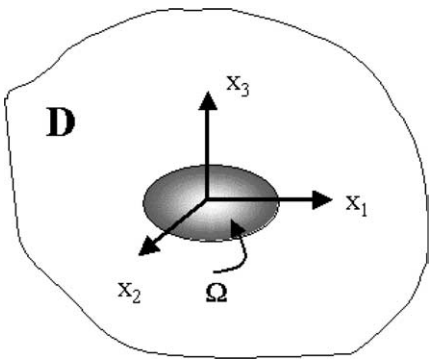

Fig. 2. An inclusion Ω confined in an infinite linear elastic chiral medium D. The origin of the coordinate system is at the center of the inclusion.

In this section, we seek to establish the general formulae for the elastic state of chiral inclusions in the presence of such eigen-deformations. Accounting for the latter prompts recasting of the constitutive laws in the usual way (Eq. (5)):

$$\begin{aligned}\boldsymbol{\sigma} &= \mathbf{a} : [\boldsymbol{\Sigma} - \boldsymbol{\Sigma}^* H(\Omega)] + \mathbf{b} : [\mathbf{K} - \mathbf{K}^* H(\Omega)] \\ \mathbf{m} &= \mathbf{b}^{\mathrm{T}} : [\boldsymbol{\Sigma} - \boldsymbol{\Sigma}^* H(\Omega)] + \mathbf{c} : [\mathbf{K} - \mathbf{K}^* H(\Omega)]\end{aligned} \tag{6a–b}$$

Here, $H(\Omega)$ is the Heaviside function on the inclusion surface, i.e.

$$H(\Omega) = \begin{cases} 1, & \mathbf{x} \in \Omega \\ 0, & \mathbf{x} \notin \Omega \end{cases} \tag{7}$$

Forming divergence of Eqs. (6), employing the kinematic relations (Eq. (1)), and the balance law (Eq. (2)) lead to the following:

$$\begin{aligned}&(\mu + \alpha)\nabla^2 \mathbf{u} + (\mu + \lambda - \alpha)\mathrm{grad}\,\mathrm{div}\,\mathbf{u} + 2\alpha \mathrm{curl}\,\boldsymbol{\phi} \\ &\quad + (\chi + \nu)\nabla^2 \boldsymbol{\phi} + (\kappa + \chi - \nu)\mathrm{grad}\,\mathrm{div}\,\boldsymbol{\phi} \\ &\quad - \underline{\{\mathbf{a} : \boldsymbol{\Sigma}^* + \mathbf{b} : \mathbf{K}^*\}\nabla H(\Omega)} + \mathbf{F} = 0 \\ &(\gamma + \varepsilon)\nabla^2 \boldsymbol{\phi} - 4\alpha\boldsymbol{\phi} + (\beta + \gamma - \varepsilon)\mathrm{grad}\,\mathrm{div}\,\boldsymbol{\phi} + 2\alpha \mathrm{curl}\,\mathbf{u} \\ &\quad + 4\nu\,\mathrm{curl}\,\boldsymbol{\phi} + (\chi + \nu)\nabla^2 \mathbf{u} + (\kappa + \chi - \nu)\mathrm{grad}\,\mathrm{div}\,\mathbf{u} \\ &\quad - \underline{\left\{\mathbf{b}^{\mathrm{T}} : \boldsymbol{\Sigma}^* + \mathbf{c} : \mathbf{K}^*\right\}\nabla H(\Omega)} + \mathbf{M} = 0\end{aligned} \tag{8a–b}$$

As has been standard in inclusion problem in both classical and enriched elastic media (Eshelby, 1957; Cheng and He, 1995; Sharma and Ganti, in press), the underlined terms in Eqs. (8) due to eigenstrains and eigentorsions can be thought of as body forces and moments respectively.

$$\begin{aligned}\mathbf{F}^* &= -\{\mathbf{a} : \boldsymbol{\Sigma}^* + \mathbf{b} : \mathbf{K}^*\}\nabla H(\Omega) \\ \mathbf{M}^* &= -\{\mathbf{b}^{\mathrm{T}} : \boldsymbol{\Sigma}^* + \mathbf{c} : \mathbf{K}^*\}\nabla H(\Omega)\end{aligned} \tag{9a–b}$$

The use of work reciprocity relations for hemitropic media allows us to solve for the elastic fields i.e.:

$$\begin{aligned}\mathbf{u}(\mathbf{x}) &= \int_V [\mathbf{G}(\mathbf{x} - \mathbf{y})\mathbf{F}(\mathbf{y}) + \boldsymbol{\Phi}(\mathbf{x} - \mathbf{y})\mathbf{M}(\mathbf{y})]\,\mathrm{d}^3 y \\ \boldsymbol{\phi}(\mathbf{x}) &= \int_V [\hat{\mathbf{G}}(\mathbf{x} - \mathbf{y})\mathbf{F}(\mathbf{y}) + \hat{\boldsymbol{\Phi}}(\mathbf{x} - \mathbf{y})\mathbf{M}(\mathbf{y})]\,\mathrm{d}^3 y\end{aligned} \tag{10a–b}$$

Here, $\mathbf{G}$ and $\boldsymbol{\Phi}$ represent the fundamental solutions (Green's functions) of the governing equations (Eqs. (5)) that yield the displacement due to a unit concentrated force and a unit concentrated couple in infinite space of a hemitropic solid. $\hat{\mathbf{G}}$ and $\hat{\boldsymbol{\Phi}}$ analogously provide solutions to the microrotation field for unit forces and moments. In matrix form, we can represent the aforementioned concepts as follows:

$$\begin{bmatrix} u_j(\mathbf{x}) \\ \phi_j(\mathbf{x}) \end{bmatrix} = \begin{bmatrix} G_{jn}(\mathbf{x} - \mathbf{y}) & \phi_{jn}(\mathbf{x} - \mathbf{y}) \\ \hat{G}_{jn}(\mathbf{x} - \mathbf{y}) & \hat{\phi}_{jn}(\mathbf{x} - \mathbf{y}) \end{bmatrix} \begin{bmatrix} f_n(\mathbf{y}) \\ m_n(\mathbf{y}) \end{bmatrix} \tag{11}$$

For the conventional centrosymmetric micropolar media, the Green's function was derived by Sandru (1966) and employed by Cheng and He (1995, 1997) in their solutions to spherical and cylindrical inclusion problem respectively. For the hemitropic case, the Green's function was presented by Nowacki (1977) and is explicitly written as follows:

$$G_{jn}(\mathbf{x}-\mathbf{y}) = \frac{1}{4\pi}\left[\frac{r_{,jn}}{2(\lambda+2\mu)} + \frac{(\kappa+2\chi)I^0_{,jn}}{(\lambda+2\mu)\Delta_0} + \frac{\varepsilon_{jik}\varepsilon_{kns}}{2}(C_0 r_{,is} + 2C_1 I^1_{,is} + 2C_2 I^2_{,is}) + \frac{\varepsilon_{jik}\varepsilon_{krs}\varepsilon_{snm}}{2} \times (D_0 r_{,irm} + 2D_1 I^1_{,irm} + 2D_2 I^2_{,irm})\right] \tag{12}$$

Some of the relevant terms that we will have occasion to refer in the main text of this paper are defined in Eq. (13). The remaining terms in Eq. (12) and a few others (in Eqs. (14)–(16)) are merely constants that are a combination of material parameters. Those are defined in Appendix A.

$$\begin{aligned} r &= |\mathbf{x}-\mathbf{y}| \\ \Delta_0 &= (\beta+2\gamma)(\lambda+2\mu) - (\kappa+2\chi)^2 \\ \Delta_1 &= (\mu+\alpha)(\gamma+\varepsilon) - (\nu+\chi)^2 \\ 1/l^2 &= 4\alpha\mu/\Delta_1 \\ I^n &= \frac{1}{\omega_n^2}\left(\frac{\mathrm{e}^{-\omega_n r}}{r} - \frac{1}{r}\right) \\ \omega_n &= \begin{cases} \sqrt{\dfrac{4\alpha(\lambda+2\mu)}{\Delta_0}}, & n=0 \\ \{\mathrm{Re}(\omega_n')|(\omega_n')^4 - (2/l^2-\tau^2)(\omega_n')^2 + 1/l^2 = 0\}, & \forall n \neq 0 \end{cases} \end{aligned} \tag{13}$$

Similarly, the other Green's functions are written in Eqs. (14)–(16):

$$\Phi_{jn}(\mathbf{x}-\mathbf{y}) = \frac{1}{4\pi}\left[-\frac{(\kappa+2\chi)I^0_{,jn}}{\Delta_0} + \varepsilon_{jik}\varepsilon_{kns}(A_1 I^1_{,is} + A_2 I^2_{,is}) + \frac{\varepsilon_{jik}\varepsilon_{krs}\varepsilon_{snm}}{2}(B_0 r_{,irm} + 2B_1 I^1_{,irm} + 2B_2 I^2_{,irm})\right] \tag{14}$$

$$\hat{G}_{jn}(\mathbf{x}-\mathbf{y}) = \frac{1}{4\pi}\left[-\frac{(\kappa+2\chi)I^0_{,jn}}{\Delta_0} + \varepsilon_{jik}\varepsilon_{kns}(\hat{C}_1 I^1_{,is} + \hat{C}_2 I^2_{,is}) + \frac{\varepsilon_{jik}\varepsilon_{krs}\varepsilon_{snm}}{2}(\hat{D}_0 r_{,irm} + 2\hat{D}_1 I^1_{,irm} + 2\hat{D}_2 I^2_{,irm})\right] \tag{15}$$

$$\hat{\Phi}_{jn}(\mathbf{x}-\mathbf{y}) = \frac{1}{4\pi}\left[-\frac{(\lambda+2\mu)I^0_{,jn}}{\Delta_0} + \varepsilon_{jik}\varepsilon_{kns}(\hat{A}_1 I^1_{,is} + \hat{A}_2 I^2_{,is}) + \varepsilon_{jik}\varepsilon_{krs}\varepsilon_{snm}(\hat{B}(I^1_{,irm} - I^2_{,irm}))\right] \tag{16}$$

Consider Eq. (10) again. Substituting expression (9) in Eq. (10) we obtain the final displacement and microrotation fields:

$$\begin{aligned} \mathbf{u}(\mathbf{x}) = \int_V &\{(\mathbf{a}:\boldsymbol{\Sigma}^* + \mathbf{b}:\mathbf{K}^*)[\nabla_y \otimes H(\Omega)]\}\mathbf{G}(\mathbf{x}-\mathbf{y}) \\ &+ \{(\mathbf{b}^{\mathrm{T}}:\boldsymbol{\Sigma}^* + \mathbf{c}:\mathbf{K}^*)[\nabla_y \otimes H(\Omega)]\}\boldsymbol{\Phi}(\mathbf{x}-\mathbf{y}) \\ &+ \{\boldsymbol{\varepsilon}:(\mathbf{a}:\boldsymbol{\Sigma}^* + \mathbf{b}:\mathbf{K}^*)\}\boldsymbol{\Phi}(\mathbf{x}-\mathbf{y})\,\mathrm{d}^3 y \\ \boldsymbol{\phi}(x) = \int_V &\{(\mathbf{a}:\boldsymbol{\Sigma}^* + \mathbf{b}:\mathbf{K}^*)[\nabla_y \otimes H(\Omega)]\}\hat{\mathbf{G}}(\mathbf{x}-\mathbf{y}) \\ &+ \{(\mathbf{b}^{\mathrm{T}}:\boldsymbol{\Sigma}^* + \mathbf{c}:\mathbf{K}^*)[\nabla_y \otimes H(\Omega)]\}\hat{\boldsymbol{\Phi}}(\mathbf{x}-\mathbf{y}) \\ &+ \{\boldsymbol{\varepsilon}:(\mathbf{a}:\boldsymbol{\Sigma}^* + \mathbf{b}:\mathbf{K}^*)\}\hat{\boldsymbol{\Phi}}(\mathbf{x}-\mathbf{y})\,\mathrm{d}^3 y \end{aligned} \tag{17a–b}$$

Terms containing gradients of the Heaviside function act as delta functions across the inclusion surface. Employing Gauss's theorem to convert these consequent surface integrals into volume integrals we obtain the following:

$$\begin{aligned}\mathbf{u}(\mathbf{x}) = &-\int_V \{(\mathbf{a}:\boldsymbol{\Sigma}^* + \mathbf{b}:\mathbf{K}^*) : [\nabla_x \otimes \mathbf{G}(\mathbf{x}-\mathbf{y}) \\ &+ (\mathbf{b}^{\mathrm{T}}:\boldsymbol{\Sigma}^* + \mathbf{c}:\mathbf{K}^*) : [\nabla_x \otimes \boldsymbol{\Phi}(\mathbf{x}-\mathbf{y})] \\ &- \{\boldsymbol{\varepsilon} : (\mathbf{a}:\boldsymbol{\Sigma}^* + \mathbf{b}:\mathbf{K}^*)\}\boldsymbol{\Phi}(\mathbf{x}-\mathbf{y})\,\mathrm{d}^3y \\ \boldsymbol{\phi}(\mathbf{x}) = &-\int_V \{(\mathbf{a}:\boldsymbol{\Sigma}^* + \mathbf{b}:\mathbf{K}^*) : [\nabla_x \otimes \hat{\mathbf{G}}(\mathbf{x}-\mathbf{y})] \\ &+ (\mathbf{b}^{\mathrm{T}}:\boldsymbol{\Sigma}^* + \mathbf{c}:\mathbf{K}^*) : [\nabla_x \otimes \hat{\boldsymbol{\Phi}}(\mathbf{x}-\mathbf{y})] \\ &+ \{\boldsymbol{\varepsilon} : (\mathbf{a}:\boldsymbol{\Sigma}^* + \mathbf{b}:\mathbf{K}^*)\}\hat{\boldsymbol{\Phi}}(\mathbf{x}-\mathbf{y})\,\mathrm{d}^3y\end{aligned} \tag{18a–b}$$

Here we have also the used the property that, $\nabla_x \mathbf{G}(\mathbf{y}-\mathbf{x}) = -\nabla_y \mathbf{G}(\mathbf{y}-\mathbf{x})$. Employing the kinematic relations we can finally write the actual strain and torsion tensor as:

$$\begin{aligned}\boldsymbol{\Sigma} &= \mathbb{S}^1 : \boldsymbol{\Sigma}^* + \mathbb{S}^2 : \mathbf{K}^* \\ \mathbf{K} &= \hat{\mathbb{S}}^1 : \boldsymbol{\Sigma}^* + \hat{\mathbb{S}}^2 : \mathbf{K}^*\end{aligned} \tag{19a–b}$$

Here $\mathbb{S}^1$, $\mathbb{S}^2$, $\hat{\mathbb{S}}^1$, $\hat{\mathbb{S}}^2$ are introduced in this article as the modified Eshelby tensors for hemitropic micropolar solids. In the following we will simply refer to them as chiral Eshelby tensors. From manipulation of Eqs. (18) assisted by kinematic relations, they can be derived to be:

$$\begin{aligned}\mathbb{S}^1_{znkl} &= a_{jikl}\Gamma_{znij} + b_{klji}P_{znij} + \varepsilon_{ijr}a_{jrkl}H_{inz} \\ \mathbb{S}_{znkl} &= b_{jikl}\Gamma_{znij} + c_{jikl}P_{znij} + \varepsilon_{ijr}b_{jrkl}H_{inz} \\ \hat{\mathbb{S}}^1_{znkl} &= -a_{jikl}\hat{\Gamma}_{injz} - b_{klji}\hat{P}_{injz} + \varepsilon_{ijr}a_{jrkl}\hat{H}_{inz} \\ \hat{\mathbb{S}}^2_{znkl} &= -b_{jikl}\hat{\Gamma}_{injz} - c_{jikl}\hat{P}_{injz} + \varepsilon_{ijr}b_{jrkl}\hat{H}_{inz}\end{aligned} \tag{20a–d}$$

The following terms are defined:

$$\begin{aligned}\Gamma_{znij} &= \varepsilon_{dzn}\mathfrak{R}^1_{idj} - \mathfrak{R}^2_{injz} \\ P_{znij} &= \varepsilon_{dzn}\mathfrak{R}^3_{idj} - \mathfrak{R}^4_{injz} \\ H_{inz} &= \mathfrak{R}^5_{inz} - \varepsilon_{dzn}\mathfrak{R}^6_{id} \\ \hat{\Gamma}_{injz} &= \mathfrak{R}^1_{inj,z} \\ \hat{P}_{injz} &= \mathfrak{R}^3_{inj,z} \\ \hat{H}_{inz} &= \mathfrak{R}^3_{inz}\end{aligned} \tag{21a–f}$$

These $\mathfrak{R}$ quantities are finally derived to be:

$$\begin{aligned}\mathfrak{R}^1_{idj} = &-\frac{(\kappa+2\chi)}{\Delta_0}\frac{\{Y_{,idj}(\omega_0) - \Pi_{,idj}\}}{\omega_0^2} + \varepsilon_{izk}\varepsilon_{kds}\left(\hat{C}_1\frac{\{Y_{,zsj}(\omega_1) - \Pi_{,zsj}\}}{\omega_1^2} + \hat{C}_2\frac{\{Y_{,zsj}(\omega_2) - \Pi_{,zsj}\}}{\omega_2^2}\right) \\ &+ \frac{\varepsilon_{izk}\varepsilon_{krs}\varepsilon_{sdm}}{2}\left(\hat{D}_0\Psi_{,zrmj} + 2\hat{D}_1\frac{\{Y_{,zrmj}(\omega_1) - \Pi_{,zrmj}\}}{\omega_1^2} + 2\hat{D}_2\frac{\{Y_{,zrmj}(\omega_2) - \Pi_{,zrmj}\}}{\omega_2^2}\right)\end{aligned} \tag{22}$$

$$\mathfrak{R}^2_{injz} = \frac{\Psi_{,injz}}{2(\lambda+2\mu)} + \frac{(\kappa+2\chi)}{(\lambda+2\mu)\Delta_0}\frac{\{Y_{,injz}(\omega_0)-\Pi_{,injz}\}}{\omega_0^2} + \frac{\varepsilon_{ivk}\varepsilon_{kns}}{2}\left(C_0\Psi_{,vsjz} + 2C_1\frac{\{Y_{,vsjz}(\omega_1)-\Pi_{,vsjz}\}}{\omega_1^2} + 2C_2\frac{\{Y_{,vsjz}(\omega_2)-\Pi_{,vsjz}\}}{\omega_2^2}\right) + \frac{\varepsilon_{ivk}\varepsilon_{krs}\varepsilon_{snm}}{2}\left(D_0\Psi_{,vrmjz} + 2D_1\frac{\{Y_{,vrmjz}(\omega_1)-\Pi_{,vrmjz}\}}{\omega_1^2} + 2D_2\frac{\{Y_{,vrmjz}(\omega_2)-\Pi_{,vrmjz}\}}{\omega_2^2}\right) \tag{23}$$

$$\mathfrak{R}^3_{idj} = \frac{(\lambda+2\mu)}{\Delta_0}\frac{\{Y_{,idj}(\omega_0)-\Pi_{,idj}\}}{\omega_0^2} + \varepsilon_{ipk}\varepsilon_{kds}\left(\hat{A}_1\frac{\{Y_{,psj}(\omega_1)-\Pi_{,psj}\}}{\omega_1^2} + \hat{A}_2\frac{\{Y_{,psj}(\omega_2)-\Pi_{,psj}\}}{\omega_2^2}\right) + \varepsilon_{ipk}\varepsilon_{krs}\varepsilon_{sdm}\hat{B}\left(\frac{\{Y_{,prmj}(\omega_1)-\Pi_{,prmj}\}}{\omega_1^2} - I^2_{,prmj}\frac{\{Y_{,prmj}(\omega_2)-\Pi_{,prmj}\}}{\omega_2^2}\right) \tag{24}$$

$$\mathfrak{R}^4_{injz} = -\frac{(\kappa+2\chi)}{\Delta_0}\frac{\{Y_{,injz}(\omega_0)-\Pi_{,injz}\}}{\omega_0^2} + \varepsilon_{itk}\varepsilon_{kns}\left(A_1\frac{\{Y_{,tsjz}(\omega_1)-\Pi_{,tsjz}\}}{\omega_1^2} + A_2\frac{\{Y_{,tsjz}(\omega_2)-\Pi_{,tsjz}\}}{\omega_2^2}\right) + \frac{\varepsilon_{itk}\varepsilon_{krs}\varepsilon_{snm}}{2}\left(B_0\Psi_{,trmjz} + 2B_1\frac{\{Y_{,trmjz}(\omega_1)-\Pi_{,trmjz}\}}{\omega_1^2} + 2B_2\frac{\{Y_{,trmjz}(\omega_2)-\Pi_{,trmjz}\}}{\omega_2^2}\right) \tag{25}$$

$$\mathfrak{R}^4_{injz} = \mathfrak{R}^5_{inj,z} \qquad \mathfrak{R}^3_{idj} = \mathfrak{R}^6_{id,j} \tag{26a–b}$$

Note from Eqs. (20)–(26) that the chiral Eshelby tensors have been cast in terms of the derivatives of certain potentials:

$$\Pi(\mathbf{x}) = \frac{1}{4\pi}\int_V \frac{1}{r}\,\mathrm{d}^3\mathbf{y} \qquad \Psi(\mathbf{x}) = \frac{1}{4\pi}\int_V r\,\mathrm{d}^3\mathbf{y} \qquad Y(\mathbf{x},\omega_n) = \frac{1}{4\pi}\int_V \frac{\mathrm{e}^{-\omega_n r}}{r}\,\mathrm{d}^3\mathbf{y} \tag{27a–c}$$

In Eq. (27), Π is the Newtonian harmonic potential, Ψ is the biharmonic potential and finally Y is the Yukawa potential. These potentials must be evaluated for the given inclusion shape and the knowledge of their derivatives completely determines the chiral Eshelby tensors and hence the solution to the elastic fields of embedded chiral inclusions. One should note that the characteristic length scale effect that appears in micropolar theories is a consequence of the Yukawa potential. Unfortunately, the limiting case (i.e. when chirality and micropolarity are absent), is difficult to extract from the expressions (19)–(27) which should, in such a limit, default to classical Eshelby tensor. The algebraic asymptotic limits are complicated by the fact that a fourth order equation has to be solved (Eq. (13)) and other degenerecies in absence of chiral effects. However, we will clearly show in Section 5 during the presentation of our numerical results that classical Eshelby's results are obtained for vanishing chirality.

4. Spherical and circular cylindrical inclusions

In the previous section we have shown that the inclusion problem in a chiral (hemitropic micropolar) solid is completely solved once the harmonic, biharmonic and Yukawa potentials for the inclusion shape are determined. For the spherical and circular cylindrical shape, explicit expressions can be developed since all three potentials and their derivatives are well documented in the literature. The harmonic and biharmonic potential and their derivatives can be found in Kellogg (1953), MacMillan (1958), Eshelby (1957, 1959, 1961) and Mura (1987). For the sake of completeness they are both recorded in Appendix B while the

reader is referred to the aforementioned reference for details on their derivatives. The Yukawa potential is considerably more difficult to evaluate but again, for the spherical and circular cylindrical shape, they have been documented in the literature on non-Newtonian gravitation fields of planets and asteroids (e.g. Gibbons and Whiting, 1981; Scherk, 1981). Generally, in the gravitational context one rarely needs more than second order derivative while in the present context up to fifth order derivatives may be needed. Higher order derivates of this potential have been presented by Cheng and He (1995, 1997) as the same potential occurs also in the centrosymmetric micropolar case. In practice though, the present author has found convenient to simply use commercially available mathematical software to directly evaluate the derivatives from the potentials listed in Appendix B. The software results were verified against explicit formulae listed in Mura (1987) for the harmonic and biharmonic case while a similar check was performed for the Yukawa potential and its derivatives against the results of Cheng and He (1995, 1997).

5. Numerical results

Perhaps the most striking example of chiral effects, in the context of inclusion problems, can be illustrated by considering a purely dilating inclusion. Under pure dilation, the solutions to micropolar elasticity problems degenerate to those of classical elasticity exhibiting no microrotations, couple stresses or size-effects. In fact Cheng and He (1995) showed analytically, that their micropolar solution for a uniformly dilating spherical inclusion coincided with that of Eshelby's classical elastic solution. In the present section we consider both spherical and circular cylindrical inclusion undergoing a purely dilatational eigenstrain. To bring out clearly the effect of chirality, eigentorsions are considered to be non-existent. Interestingly, in several physical problems of interest, the naturally occurring eigenstrains are also dilatational in nature (e.g. lattice mismatch and thermal expansion).

The strain and torsion behavior in both spherical and circular cylindrical inclusions are shown as a function of position in Figs. 3 and 4 respectively. The curves are plotted for different values of chirality. In all the graphs, the trace of the strain or torsion tensor is plotted. The results are contrasted with both classical elasticity result as well as micropolar results (which of course are identical for this particular

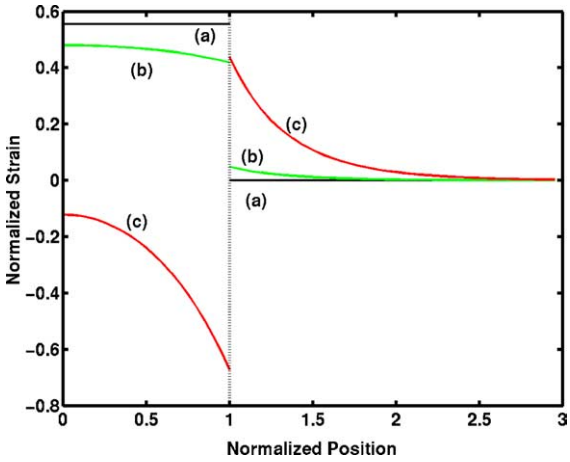

Fig. 3. Spherical inclusion. To normalize the results, the actual strain is multiplied by $1/3\varepsilon^*$ while the position is normalized with respect to the inclusion radius. Results are plotted for a fixed characteristic length of $a\omega_0 = 2$ and a Poisson ratio of 0.25 (a) classical and micropolar results which are both identical in this case; $c_h = 0$, (b) $c_h = 0.5$ and (c) $c_h = 0.9$.

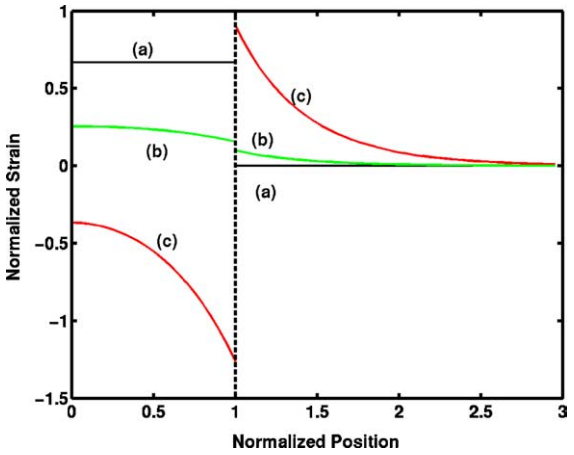

Fig. 4. Cylindrical inclusion. To normalize the results, the actual strain is multiplied by $1/2\varepsilon^*$ while the position is normalized with respect to the inclusion radius. Results are plotted for a fixed characteristic length of $a\omega_0 = 2$ and a Poisson ratio of 0.25 (a) classical and micropolar results which are both identical in this case; $c_h = 0$, (b) $c_h = 0.5$ and (c) $c_h = 0.9$.

problem). Wherever applicable, position is normalized with respect to inclusion radius, "a" (i.e. inclusion–matrix interface coordinate is 1) and inclusion radius is normalized by multiplication with ω_0. To suitably interpret our numerical results our definition of chirality and a few words on the material parameters are also in order.

All results are plotted for a fixed Poisson's ratio of 0.25 (all figures) and inclusion size, $\omega_0 a = 2$ (Figs. 3–5). For simplicity (and without loss of the essence of isotropic chirality), it is assumed that the chiral material constants are related by, $\chi = \kappa$, $\nu = 0$. This condition (which is thermodynamically admissible) simplifies presentation of numerical results in terms of only one chirality parameter (to be discussed

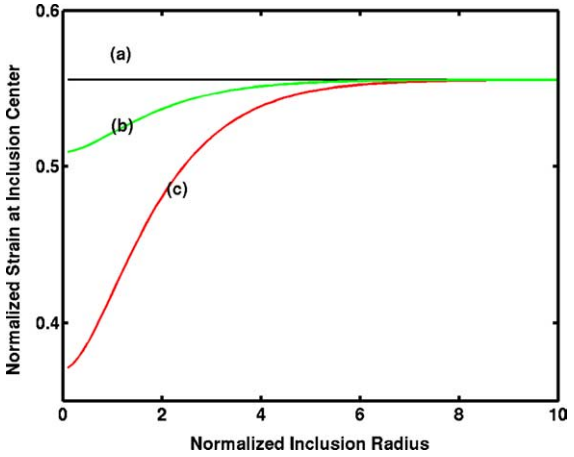

Fig. 5. Spherical inclusion. To normalize the results, the actual strain is multiplied by $1/3\varepsilon^*$ while the inclusion radius is normalized with respect to the characteristic length: $1/\omega_0$. Results are plotted for a fixed Poisson ratio of 0.25 (a) classical and micropolar results which are both identical in this case; $c_h = 0$, (b) $c_h = 0.2$ and (c) $c_h = 0.5$.

shortly). With the adopted assumptions regarding the material constants, the most natural definition of "chirality" that emerges is:

$$c_h = \frac{9\chi^2}{(\beta + 2\gamma)(\lambda + 2\mu)} \tag{28}$$

Based on thermodynamic considerations (Lakes, 1981; Nowacki, 1986) one can deduce that the chirality, c_h as defined in Eq. (28) can only vary between 0 and 1. Absence of chirality i.e. $c_h = 0$ indicates a perfectly centrosymmetric material i.e. classical elastic or centrosymmetric micropolar solid. In Figs. 3 and 4, the elastic state both internal and exterior to the inclusion is presented. As expected, the strain undergoes a jump across the inclusion interface. As well known in classical elasticity, a purely dilating circular or spherical inclusion has zero dilation exterior to the inclusion. We recover this result (Figs. 3 and 4) by letting $c_h \to 0$. Of course, the most striking feature of the results depicted in Figs. 3 and 4 is the inhomogeneous nature of the strain within the inclusion in contrast to the well-recognized uniform classical strain (Eshelby, 1957). Interestingly, chirality appears to lower the strain and for high enough chirality a reversal of sign occurs (i.e. compression to tension and vice-versa). There is an important consequence of the fact that chirality appears to lower the apparent classical strain (obviously, part of the energy diverting to torsion degrees of freedom). For a composite consisting of chiral inclusions, the *apparent* effective bulk modulus predicted by using the present work will be stiffer as compared to the equivalent classical no-chiral results. The details of a homogenization process based on the present work are beyond its scope and will be presented elsewhere.

In the preceding figures, the size-effect is not apparent since the results were plotted for fixed inclusion size but varying chirality. To illustrate size-dependency of the chiral solution, the strain at the center of the spherical and cylindrical inclusion is plotted (Figs. 5 and 6) with respect to the normalized inclusion radius for different chiralities. Since classical elasticity is size-independent, no variation should be observed for that case. As patent, the chiral inclusion does indeed exhibit a distinct size-effect. Asymptotically, regardless of the chirality, as the inclusion size is increased much larger than the characteristic length scale ($1/\omega_0$), the elastic fields approach the classical solutions (i.e. torsions and hence moment stresses disappear).

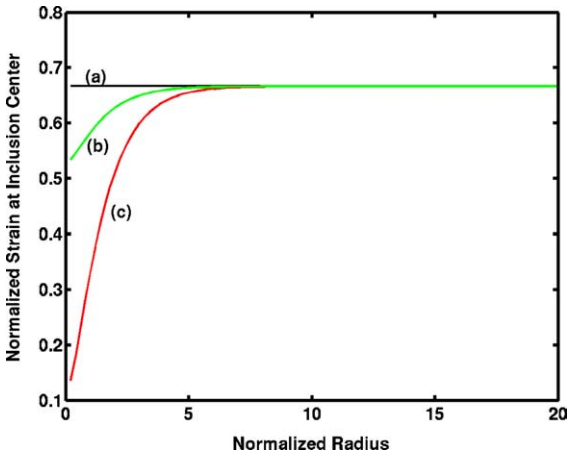

Fig. 6. Cylindrical inclusion. To normalize the results, the actual strain is multiplied by $1/2\varepsilon^*$ while the inclusion radius is normalized with respect to the characteristic length: $1/\omega_0$. Results are plotted for a fixed Poisson ratio of 0.25 (a) classical and micropolar results which are both identical in this case; $c_h = 0$, (b) $c_h = 0.2$ and (c) $c_h = 0.5$.

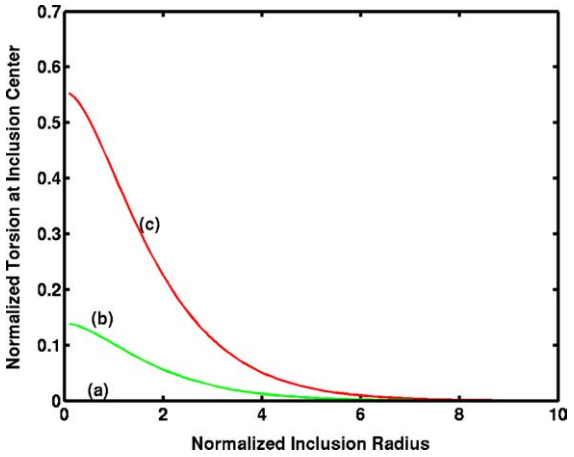

Fig. 7. Spherical inclusion. To normalize the results, the actual curvature is multiplied by $-2\chi/(\lambda+2\mu)\varepsilon^*$ while the inclusion radius is normalized with respect to the characteristic length: $1/\omega_0$. Results are plotted for a fixed Poisson ratio of 0.25 (a) classical and micropolar results which are both identical in this case; $c_h = 0$, (b) $c_h = 0.2$ and (c) $c_h = 0.5$.

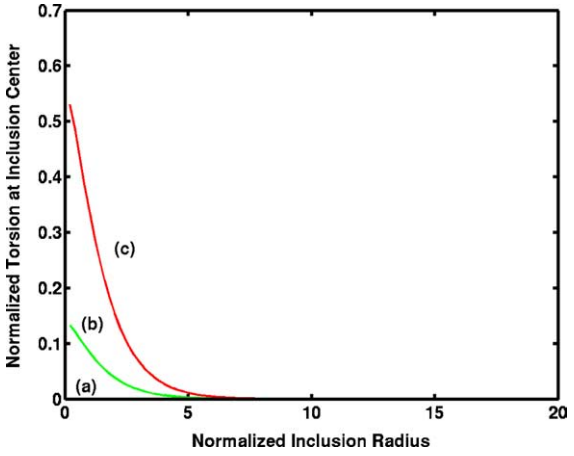

Fig. 8. Cylindrical inclusion. To normalize the results, the actual strain is multiplied by $2\chi/(\lambda+2\mu)\varepsilon^*$ while the inclusion radius is normalized with respect to the characteristic length: $1/\omega_0$. Results are plotted for a fixed Poisson ratio of 0.25 (a) classical and micropolar results which are both identical in this case; $c_h = 0$, (b) $c_h = 0.2$ and (c) $c_h = 0.5$.

Figs. 7 and 8 are, however, the most dramatic since they clearly show presence of torsion otherwise absent in non-chiral solids. These figures represent the torsion behavior for spherical and cylindrical inclusions respectively. One would expect such behavior form cylindrically-shaped helical inclusions or coiled structure (say in the shape of a sphere) thus making the present formalism extremely useful for biological media and other complex materials exhibiting axial–twist coupling.

As evident from Figs. 7 and 8, torsions disappear for large inclusions sizes (typically $>5a\omega_0$) regardless of the value of chirality.

For practical applications, one requires accurate assessment of the various centrosymmetric micropolar and the chiral material properties. While in depth discussion of this issue is beyond the scope of the present

work, we have provided a brief summary of means and methods to characterize micropolar properties in Appendix C.

6. Summary and conclusions

In summary, we have extended Eshelby's classical approach towards inclusions to incorporate the effect of chirality via the concept of a hemitropic micropolar media. An additional consequence of this approach is that the resulting chiral elastic state of inclusions is rendered size-dependent. Apart from the general formalism, explicit expressions were constructed for spherical and infinite circular cylindrical inclusion. Unlike the classical solutions the elastic state within the chiral spherical and circular cylindrical inclusions was found to be inhomogeneous. Numerical results for the case of pure dilatation were presented in which the centrosymmetric micropolar theory and the classical elasticity theory yield identical results and are thus size-independent. For the same problem, our chiral solutions however, predict the presence of size-dependent torsions and significant differences in strain profiles. As the inclusion size is increased appreciably larger than the characteristic micropolar length scale, regardless of the level of the chirality, classical solution is recovered.

As in previous works on the inclusion problem in enriched elasticity (e.g. Cheng and He, 1995, 1997), in the present work, only Eshelby's first problem was tackled. The inhomogeneity problem (Eshelby's second problem) has no simple solution in this case due to the non-uniform nature of the chiral Eshelby tensors (even for the ellipsoidal family). Nevertheless, approximate solutions to effective chiral properties of materials containing inhomogeneities can most likely be constructed following a perturbation type approach. Recently, for centrosymmetric micropolar elasticity, Sharma and Dasgupta (2002) presented such an approach whereby they employed the first term of such a perturbation series that simply involved averaging of the micropolar Eshelby tensors derived by Cheng and He (1995, 1997). Such an extension of the present paper is relegated to a future work.

Appendix A. Definition of some terms in Eqs. (12), (14)–(16)

The remaining constants occurring in Eqs. (12), (14)–(16) and not defined in the main text are listed below (Nowacki, 1977):

$$A_n = \frac{(\chi+\nu)(\omega_n^2 - 1/l^2) - 2\alpha\tau}{\omega_1^2 - \omega_2^2}$$

$$B_n = \begin{cases} -\dfrac{2\alpha}{l^2\omega_1^2\omega_2^2}, & n=0 \\ \dfrac{[2\alpha - \tau(\chi+\nu)]\omega_n^2 - 2\alpha/l^2}{\omega_n^2(\omega_1^2-\omega_2^2)} \end{cases} \tag{A.1}$$

$$C_n = \begin{cases} -\dfrac{4\alpha}{l^2\omega_1^2\omega_2^2}, & n=0 \\ \dfrac{[(\gamma+\varepsilon)/l^2 + 4\nu\tau + 4\alpha]\omega_n^2 - 4\alpha/l^2 - (\gamma+\varepsilon)\omega_n^4}{\omega_n^2(\omega_1^2-\omega_2^2)} \end{cases}$$

$$D_n = \begin{cases} -\dfrac{4(\alpha+\nu/l^2)}{l^2\omega_1^2\omega_2^2}, & n=0 \\ \dfrac{[(\gamma+\varepsilon)\tau + 4\nu]\omega_n^2 - 4(\nu/l^2+\alpha)}{\omega_n^2(\omega_1^2-\omega_2^2)} \end{cases} \tag{A.2}$$

$$\hat{B} = \frac{\tau(\mu+\alpha)}{\omega_1^2-\omega_2^2}$$
$$\hat{A}_n = \frac{(\mu+\alpha)(1/l^2-\omega_n^2)}{\omega_1^2-\omega_2^2}$$
$$\hat{C}_n = \frac{(\chi+\nu)(\omega_n^2-1/l^2)-2\alpha\tau}{\omega_1^2-\omega_2^2} \tag{A.3}$$
$$\hat{D}_n = \begin{cases} -\dfrac{2\alpha}{l^2\omega_1^2\omega_2^2}, & n=0 \\ \dfrac{[2\alpha-(\chi+\nu)\tau]\omega_n^2-2\alpha/l^2}{\omega_n^2(\omega_1^2-\omega_2^2)} \end{cases}$$

Appendix B. Harmonic, biharmonic and Yukawa potentials for spheres and circular cylinder

The harmonic and biharmonic potentials for the sphere is given below (Eshelby, 1957, 1959; Mura, 1987). The expression for cylinder is excessively long (especially outside the inclusion) and can be directly obtained from (Mura, 1987).

$x = |\mathbf{x}|$

Sphere:

$$\Pi = \begin{cases} \dfrac{1}{6}(3a^2-x^2), & \mathbf{x}\in\Omega \\ \dfrac{a^3}{3x}, & \mathbf{x}\notin\Omega \end{cases} \tag{B.1}$$
$$\Psi = \begin{cases} \dfrac{1}{12}(3a^4+2a^2x^2-\dfrac{x^4}{5}), & \mathbf{x}\in\Omega \\ \dfrac{a^3}{3x}(x^2+\dfrac{a^2}{5}), & \mathbf{x}\notin\Omega \end{cases}$$

Here, "a" is the inclusion radius. The Yukawa potentials are (Cheng and He, 1995, 1997; Gibbons and Whiting, 19; Scherk, 1981)

Sphere:

$$Y = \begin{cases} \dfrac{1}{\omega_n^2}\left\{1-\left(\dfrac{1}{\omega_n}+a\right)e^{-\omega_n x}\dfrac{\sinh\omega_n x}{x}\right\}, & \mathbf{x}\in\Omega \\ \dfrac{1}{\omega_n^2}\left(a\cosh\omega_n x-\dfrac{1}{\omega_n}\sinh\omega_n x\dfrac{e^{-\omega_n x}}{x}\right), & \mathbf{x}\notin\Omega \end{cases} \tag{B.2}$$

Circular cylinder:

$$Y = \begin{cases} \dfrac{1}{\omega_n}\{xI_1(\omega_n x)K_0(\omega_n x)+xI_0(\omega_n x)K_1(\omega_n x)-aI_0(\omega_n x)K_1(\omega_n a)\}, & \mathbf{x}\in\Omega \\ \dfrac{a}{\omega_n}I_1(\omega_n a)K_0(\omega_n x), & \mathbf{x}\notin\Omega \end{cases}$$

K_0 and K_1 refer to modified Bessel function of the second kind (of orders 0 and 1 respectively).

Appendix C. Discussion on determination of centrosymmetric micropolar and hemitropic micropolar material constants

Hemitropic micropolar material constants (or isotropic chiral parameters) manifest their presence in phonon dispersion curves. More specifically, as indicated by Eringen (1999), the optical branch of the phonon dispersion curve can be employed to determine some of the material parameters. Recently, in a sequence of works, Chen et al. (2003) and Chen and Lee (2003) have laid down the methodology to determine these various micromorphic parameters. While they did not explicitly tackle chiral materials (only their centro-symmetric counterparts), their methodology could be indeed employed to do so. Regarding size-dependency (or characteristic length scales), early experimental attempts by Jashman and Gauthier (1982) on epoxy-aluminum particulate composites revealed a characteristic length scale nearly equal to particle radius. Experiments by Yang and Lakes (1982) on human compact bones indicated a characteristic length scale of roughly $\sim$0.2 mm. In a separate paper, Lakes (1981) specifically discusses chirality in human bones. From his work, roughly speaking (in our terminology), bones have a chirality of 15%. In artificial composites containing twisted fibers, using a quantitative mode of a rod under tension, one could relate the ensuing twist (under tension) of some of the chiral properties (see, Lakes, 2001). Clearly though, much further experimental work is need in the determination of chiral and micropolar properties. Since experimental determination of these properties has been extremely challenging, a promising avenue may be the employment of atomistic methods.

References

Bilby, B.A., Miller, K.J., Willis, J.R., 1984. IUTAM/IFC/ICM Symposium on Fundamentals of Deformation and Fracture (Eshelby Memorial Symposium, Sheffield, England, 2–5 April 1984), Cambridge University Press, Cambridge.

Chen, Y., Lee, J.D., Eskandarian, A., 2003. Examining the physical foundation of continuum theories from the viewpoint of phonon dispersion relation. International Journal of Engineering Science 41 (1), 61–83.

Chen, Y., Lee, J.D., 2003. Determining material constants in micromorphic theory through phonon dispersion relations. International Journal of Engineering Science 41 (8), 871–886.

Cheng, Z.Q., He, L.H., 1995. Micropolar elastic fields due to a spherical inclusion. International Journal of Engineering Science 33 (3), 389–397.

Cheng, Z.Q., He, L.H., 1997. Micropolar elastic fields due to a circular cylindrical inclusion. International Journal Of Engineering Science 35 (7), 659–668.

Eringen, A.C., 1999. Microcontinuum Field Theories. I: Foundations and Solids. Springer-Verlag, New York.

Eshelby, J.D., 1957. The determination of the elastic field of an ellipsoidal inclusion and related problems. Proceedings of the Royal Society of London A A241, 376–396.

Eshelby, J.D., 1959. The elastic field outside an ellipsoidal inclusion. Proceedings of the Royal Society of London A A252, 561–569.

Eshelby, J.D., 1961. Elastic inclusions and inhomogeneities. In: Sneddon, I.N., Hill, R. (Eds.), Progress in Solid Mechanics, vol. 2. North Holland, Amsterdam, pp. 89–140.

Gibbons, G.W., Whiting, B.F., 1981. Newtonian gravity measurements impose constraints on unification theories. Nature 291, 636.

Haijun, Z., Zhong-can, O., 1998. Bending and twisting elasticity: A revised Marko–Siggia model on DNA chirality. Physical Review E 58 (4), 4816.

Harris, P.J.F., 2002. Carbon Nanotubes and Related Structures. Cambridge University Press.

Jashman, W.E., Gauthier, R.D., 1982. Dynamics measurements of micropolar elastic constants. In: Kroner, E., Anthony, K.H. (Eds.), Continuum Models of Discrete Systems, vol. 3. University of Waterloo Press, Ontario, Canada.

Kellogg, O.D., 1953. Foundation of Potential Theory. Dover, New York.

Lakes, R.S., 1981. Is Bone Elastically Noncentrosymmetric? 34th ACEMB, Houston Texas, September 21–23.

Lakes, R.S., 2001. Elastic and viscoelastic behaviour of chiral materials. International Journal of Mechanical Sciences 43, 1579–1589.

Lakes, R.S., Benedict, R.L., 1982. Noncentrosymmetry in micropolar elasticity. International Journal of Engineering Science 29, 1161.

Lakhtakia, A., Varadan, V.K., Varadan, V.V., 1988. Elastic wave propagation in noncentrosymmetric, isotropic media: Dispersion and field equations. Journal of Applied Physics 64, 5246.

Lakhtakia, A., 2002. Microscopic model for elastostatic and elastodynamic excitation of chiral sculptured thin films. Journal of Composite Materials 36 (11), 1277.

MacMillan, W.D., 1958. The Theory of the Potential. Dover, New York.
Marder, M.P., 2000. Condensed Matter Physics. Wiley-Interscience, NY.
Markov, K., Preziosi, L., 2000. Heterogeneous Media: Micromechanics Modeling Methods and Simulations. Birkhauser Verlag, Switzerland.
McCall, M.W., Lakhtakia, A., Weiglhofer, W.S., 2002. The negative index of refraction demystified. European Journal of Physics 23, 353–359.
Mura, T., 1987. Micromechanics of Defects in Solids. Martinus Nijhoff, Hague, Netherlands.
Mura, T., Shodja, H.M., Hirose, Y., 1996. Inclusion problems. Applied Mechanics Review 49 (10, part 2), S118–S127.
Mura, T., 2000. Some new problems in the micromechanics. Materials Science and Engineering A (Structural Materials: Properties, Microstructure and Processing) A285 (1–2), 224–228.
Nowacki, J.P., 1977. Green's function for a hemitropic micropolar continuum. Bulletin De L'Academie Polonaise Des Sciences XXV (8), 235.
Nowacki, W., 1986. Theory of Asymmetric Elasticity. Polish-Scientific Publishers, Warszawa and Pergamon Press.
Ro, R., 1999. Elastic activity of the chiral medium. Journal of Applied Physics 85 (5), 2508.
Robbie, K., Brett, M.J., Lakhtakia, A., 1996. Chiral sculpted thin films. Nature 384, 616.
Sandru, N., 1966. One some problems of the linear theory of the asymmetric elasticity. International Journal of Engineering Science 4 (1), 81.
Scherk, J., 1981. In: Ferrara, S., Ellis, J., Van Nieuwenhuizen, P. (Eds.), Unification of the Fundamental Particle Interactions. Plenum, NY.
Sharma, P., Dasgupta, A., 2002. Scale-dependent average elastic fields of spherical and cylindrical inhomogeneities in micropolar medium and overall properties. Physical Review B 66, 2241X.
Sharma, P., Ganti, S., in press. Size-dependent Eshelby's tensor for embedded nano-inclusions incorporating surface/interface energies. Journal of Applied Mechanics.
Smith, D.R., Padilla, W.J., Vier, D.C., Nemat-Nasser, S.C., Schultz, S., 2000. Composite medium with simultaneously negative permeability and permittivity. Physical Review Letters 84, 4184.
Yang, J.F.C., Lakes, R.S., 1982. Experimental study of micropolar and couple stress elasticity in compact bone bending. Journal of Biomechanics 15 (2), 91–98.